

IAC-12-C1.4.8

HIGH AREA-TO-MASS RATIO HYBRID PROPULSION EARTH TO MOON TRANSFERS IN THE CR3BP

Willem Johan van der Weg
University of Strathclyde, United Kingdom, willem.van-der-weg@strath.ac.uk

Massimiliano Vasile
University of Strathclyde, United Kingdom, massimiliano.vasile@strath.ac.uk

This paper examines the design of transfers that are useful to micro or nano spacecraft with high area-to-mass ratio, propelled by a simple propulsion engine (such as chemical with a specific impulse ca. 100 to 300 s or arcjet/resistojet), and possessing relatively small solar reflective panels to provide power and a small thrust due to solar radiation pressure. This type of transfer is becoming of greater interest as advances in structures, materials, and small spacecraft design & propulsion are made. Such a hybrid design especially offers possibilities of cheaply exploring the Moon using multiple vehicles. With this small hybrid design, interior transfers in the circular restricted 3-body problem between the pair of primary and secondary masses (e.g. the Earth and Moon) are attempted using solar radiation pressure and multiple small impulses. The source of the outside solar radiation pressure is modeled using an external source rotating about – and in the plane of – the co-rotating set of primary and secondary masses. Starting from a GTO about the primary mass a basic optimization method of sequences of manoeuvres is used to achieve the transfer, where the segments are patched together using ideally small maneuvers. The spacecraft coasting arc is controlled by a number of locally optimal control laws to optimize performance while minimizing computational cost. The spacecraft hops onto a stable invariant manifold leading to the system's Lagrange L1 point after successive small maneuvers and coasting arcs. Following connection with a manifold and subsequent arrival at a periodic orbit at L1, temporary or permanent capture around the Moon can be performed using the remaining resources at hand.

I. INTRODUCTION

The increasing miniaturization of spacecraft engines and other components combined with the expanding capabilities of small lightweight systems has led to a number of interesting avenues of exploration for novel missions with low associated cost. This doctrine is applied here to obtain a preliminary design for a transfer to the Moon using cheap high area-to-mass ratio hybrid propulsion spacecraft. The spacecraft is propelled by a simple chemical or electrical system and is equipped with relatively small reflective panels to provide power and a small thrust due to solar radiation pressure. Such a hybrid design is suited for exploration of the Moon using multiple cheap vehicles.

Section II provides an explanation of the dynamic model used to design the transfers. Section III gives a brief explanation of the design process employed. Section IV shows some of the results that have been obtained so far. A small study of spacecraft lunar orbit longevity for a variety of initial conditions is shown in section V. Finally, section VI contains some discussion and conclusion.

II. SYSTEM MODEL

A modified version of the standard circular restricted 3-body problem (CR3BP) is employed to study the duration and propellant cost of interior Earth – Moon transfers that can be flown by this hybrid class of spacecraft. The equations found in this section follow the work previously done by Simo and McInnes[1]. Here it is defined that the larger primary m_1 is the Earth and the smaller primary m_2 is the Moon. The two primaries move about their centre of mass in a circular orbit while the third body is of negligible mass to be able to influence the movement of the two primaries (cf. Fig. I).

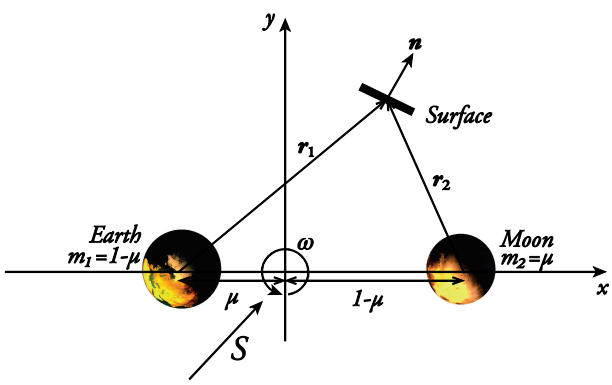

Fig. I: Schematic geometry of circular restricted 3-body problem (z-axis pointing out from paper).

The equations of motion are provided here for a synodic reference frame in dimensionless coordinates for greatest generality. As by standard convention the total mass of the system is a unit mass ($m_1 + m_2 = 1$) and the

constant separation between both primaries is a unit length. The normalized mass of both primaries then follows as $m_1 = 1 - \mu$ and $m_2 = \mu$. The equations of motion in vector form are

$$\frac{d^2\boldsymbol{r}}{dt^2} + 2\boldsymbol{\omega} \times \frac{d\boldsymbol{r}}{dt} + \nabla U(\boldsymbol{r}) = \boldsymbol{a}, \qquad [1]$$

where $\boldsymbol{r}$ is the position vector of the third body and $\boldsymbol{a}$ is the introduced acceleration solar radiation pressure (the term on the right would be zero for a standard CR3BP definition taking into account only the gravitational accelerations from the two primaries). The angular velocity vector $\boldsymbol{\omega}$ of the rotating frame is defined as

$$\boldsymbol{\omega} = \omega e_z, \qquad [2]$$

where e_z is the unit vector of the z axis. The 3-body gravitational potential is defined by

$$U(\boldsymbol{r}) = -\left(\frac{1}{2}|\omega \times \boldsymbol{r}|^2 + \frac{1-\mu}{r_1} + \frac{\mu}{r_2}\right), \qquad [3]$$

where μ is the mass ratio for the Earth-Moon system (μ = 0.01215) and the third body positions w.r.t. the Earth primary $\boldsymbol{r}_1$ and Moon primary $\boldsymbol{r}_2$ are

$$\begin{aligned} \boldsymbol{r}_1 &= [x+\mu, y, z], \\ \boldsymbol{r}_2 &= [x+\mu-1, y, z]. \end{aligned} \qquad [4]$$

The acceleration due to the solar radiation pressure is defined as

$$\boldsymbol{a} = a_0(\boldsymbol{S}\cdot\boldsymbol{n})^2\boldsymbol{n}, \qquad [5]$$

where a_0 is the magnitude of the solar radiation pressure acceleration, $\boldsymbol{n}$ is the unit vector normal to the surface of the reflective surface of the spacecraft, and $\boldsymbol{S}$ is the direction vector of sunlight given by

$$\boldsymbol{S} = [\cos(w_s t + S_0) \quad -\sin(w_s t + S_0) \quad 0], \qquad [6]$$

where ω_s is the angular rate of the sunlight vector in the synodic reference frame. S_0 represents the initial direction of the sunlight at t_0 (if this term is omitted the direction of sunlight is initially directly along the axis of the primaries from the larger primary Earth to the smaller primary). The angular rate of the sunlight vector ω_s can be determined by subtracting the dimensionless value of the rotation rate of the Earth about the Sun from the rotation rate of the Moon about the Earth (equal to unity in the dimensionless system), obtaining ω_s = 0.923 as the angular rate of the sunlight in the dimensionless synodic reference frame.

II.I Reflective Surface Pointing

The reflective surface is controlled using a locally optimal control law obtained from maximising the change in velocity along the velocity vector of the spacecraft. This is derived from studying the geometry of the surface and incoming sunlight vector[2], and can be written as

$$\beta = \operatorname{atan}\left(\frac{3\tan\alpha}{4} + \frac{\sqrt{9\tan^2\alpha + 8}}{4}\right). \qquad [7]$$

The angle α is defined as

$$\alpha = \operatorname{acos}(\boldsymbol{e}_v \cdot \boldsymbol{S}) - \frac{\pi}{2}, \qquad [8]$$

where $\boldsymbol{e}_v$ and $\boldsymbol{S}$ represent the unit vector of velocity of the spacecraft and the unit vector of the sunlight direction, respectively. To maximise the local increase of energy the unit vector $\boldsymbol{n}$ (defining the spacecraft's surface pointing), is then aligned by rotating the sunlight unit vector $\boldsymbol{S}$ by the angle β about the rotation axis defined by the normal vector of the plane spanned by the spacecraft velocity vector $\boldsymbol{e}_v$ and the sunlight unit vector $\boldsymbol{S}$. To maximise the local decrease of energy the rotation is simply in the opposite direction, i.e. $-\beta$.

III. TRANSFER DESIGN

Suitable transfers between Earth and Moon were sought by attempting to insert the spacecraft into a halo orbit at the Earth – Moon L1 libration point. Then from the halo orbit an attempt is made to become captured by the Moon into some form of quasi-periodic orbit. This effectively divides the problem into two steps, both originating at the halo orbit: a backwards in time propagation from the halo orbit to some form of orbit about the Earth, and a forwards in time propagation that leads to capture about the Moon.

III.I Spacecraft Parameters

For the purposes of this study we assumed a number of parameters for 2 hypothetical spacecraft, a high performance one and a perhaps more realistic low cost spacecraft. These listed in Table I.

High Performance S/C		
Specific Impulse	4500	[*s*]
Thrust Level	10	[*mN*]
Wet Mass	4	[*kg*]
Area To Mass Ratio	2 ~ 6	[–]
Low Cost S/C		
Specific Impulse	4500	[*s*]
Thrust Level	1.6	[*mN*]
Wet Mass	4	[*kg*]
Area To Mass Ratio	0.5 ~ 1	[–]

Table I: List of spacecraft parameters used in this study.

III.II Halo orbit Selection

To keep the entire problem planar a family of halo orbits was generated[3,4] that lie in the *x-y* plane (the rotation plane of the primaries). Three of these are selected to serve as reference orbits to connect trajectories from the Earth. Samples of the generated family, as well as the selected orbits (marked in red), are shown in Fig. II.

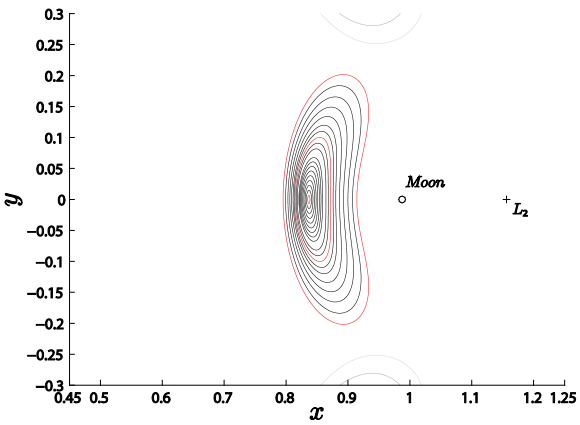

Fig. II: Family of planar halo orbits (selected halo orbits in red).

The 3 selected orbits are then used as starting points for the propagation forwards toward the Moon and the propagation backwards towards the Earth.

III.III Backward Propagation towards the Earth

The initial conditions for propagating backwards from halo orbit towards the Earth are obtained in the same exact manner that the initial conditions to create the invariant manifolds[5] are obtained. An example set of stable and unstable manifolds, along with their direction of motion, is provided in Fig. III.

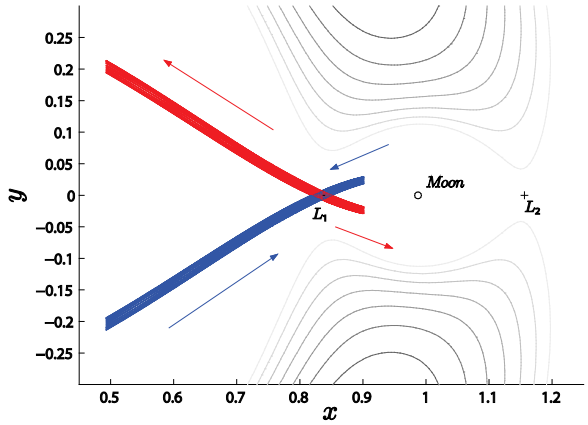

Fig. III: An example set of invariant manifolds for the Earth-Moon system (blue is stable, and red is unstable).

The stable manifold leading towards the Earth is then propagated backwards in time for a set amount of time where the reflective surface is pointed such that the energy of the spacecraft is decreased as time moves forward (i.e. the energy is increased as time moves forward after leaving the Earth).

III.IV Backward Propagation Manoeuvres

Once the set period of coasting is completed a series of small manoeuvres are performed in order to connect the initial Earth orbit and the state obtained from coasting backwards in time from the halo orbit. The reason that a set coasting time is introduced after all manoeuvres are performed to depart from the Earth and insert into halo orbit are twofold: the optimization process is simplified by separating these two sections of the design, and the energy increase will generally be greater after manoeuvres have been performed as the velocity increase due to the reflective surface is relatively greater than the velocity of the spacecraft when it is further out from the Earth.

If during the coasting period the spacecraft goes past the L1 libration point back into the vicinity of the Moon successive small manoeuvres are performed such that this does not occur.

The manoeuvres are simplified to small impulsive small manoeuvres instead of finite thrusting arcs. The high performance spacecraft can perform manoeuvres of up to 30 m/s while the low cost spacecraft can perform manoeuvres of up to 5 m/s at a single point.

III.V Initial Earth Orbit

The initial Earth orbit is a standard GTO in the *x-y* plane of the problem for the high performance spacecraft. To avoid excessive radiation in the case of the low cost spacecraft, it is propelled constantly by its small low thrust engine for close to 54 days until a perigee of GEO is reached. This manoeuvre costs a total of almost 1.9 km/s to perform, equivalent to a

propellant mass of 0.17 kg. The resulting outward spiral is shown in Fig. IV.

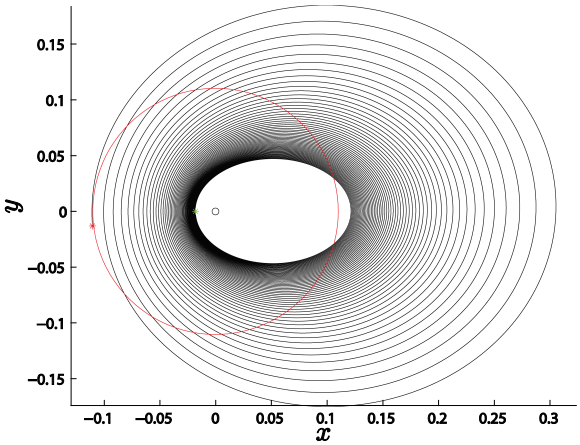

Fig. IV: Trajectory of the spacecraft from GTO to GEO perigee altitude in non-dimensional inertial reference frame.

III.VI Forward Propagation and Capture

The final section of the transfer is then the departure from Halo orbit towards the Moon. Here, the reflective surface is used to reduce energy to facilitate capture. Depending on the size of the targeted halo orbit, manoeuvres can be used to reduce the energy further such that the spacecraft can be captured. Capture becomes increasingly expensive in terms of manoeuvres (depending also on the selected area-to-mass ratio of the spacecraft) as the size of the halo orbit increases. For all halo orbits, a trajectory can be selected such that lunar impact occurs.

III.VII Transfer Optimisation

For the optimisation of the transfers the initial conditions are the halo orbit size, the selection of the particular manifold from the halo orbit, the initial orbit size around the Earth, and the request sailing time.

The position or timing of each manoeuvre is not optimized separately. Rather, to increase simplicity greatly, manoeuvres are grouped into sequences of either perigee or apogee controlling manoeuvres located at minimum or maximum locations of the orbit (w.r.t. the Earth). Speaking from the perspective of the backwards in time propagation from the halo orbit, it was found that generally it is effective to place a sequence of apogee lowering manoeuvres, followed by a sequence of perigee lowering manoeuvres before lowering apogee again in order to connect to the initial orbit at Earth.

IV. RESULTS

This section presents the results found for both the high performance and low cost spacecraft.

IV.I High Performance Spacecraft

Using the above method to find possible transfers, a number of manifold lines on the manifold tube are used to attempt connection between halo and Earth GTO. Fig. V shows the resulting Δv costs for a connection between Earth GTO and a small planar halo orbit.

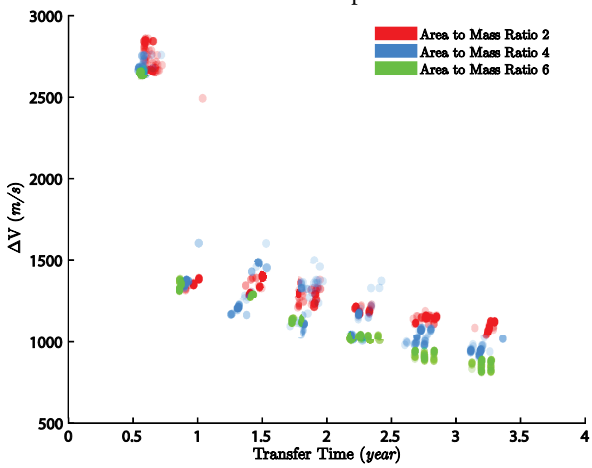

Fig. V: Δv as a function of total transfer time of the solutions found for the small halo orbit.

The lowest scoring candidates for the small halo orbit for varying sailing periods and area-to-mass ratios are given in Table II in m/s.

Sailing Period	AMR 2	AMR 4	AMR 6
0	2,657	2,644	2,641
0.5	1,342	1,357	1,339
1.0	1,303	1,189	1,294
1.5	1,233	1,085	1,144
2.0	1,188	1,037	1,042
2.5	1,138	1,003	919
3.0	1,063	937	855

Table II: Lowest Δv solutions found for the small halo orbit.

Fig. VI shows the resulting Δv costs for a connection between Earth GTO and a medium planar Halo orbit.

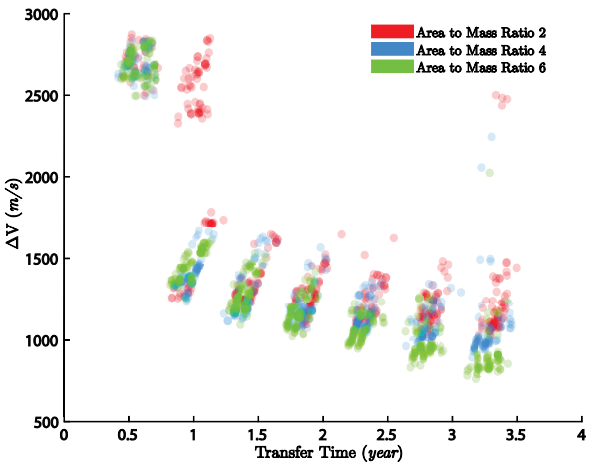

Fig. VI: Δv as a function of total transfer time of the solutions found for the medium halo orbit.

The lowest scoring candidates for the medium halo orbit for varying sailing periods and area-to-mass ratios are given in Table III in m/s.

Sailing Period	AMR 2	4	6
0	2,504	2,498	2,501
0.5	1,261	1,246	1,261
1.0	1,180	1,117	1,096
1.5	1,090	1,075	1,030
2.0	1,075	1,002	950
2.5	1,016	954	836
3.0	996	893	764

Table III: Lowest Δv solution found for the medium halo orbit.

Fig. VII shows the resulting Δv costs for a connection between Earth GTO and a large planar halo orbit.

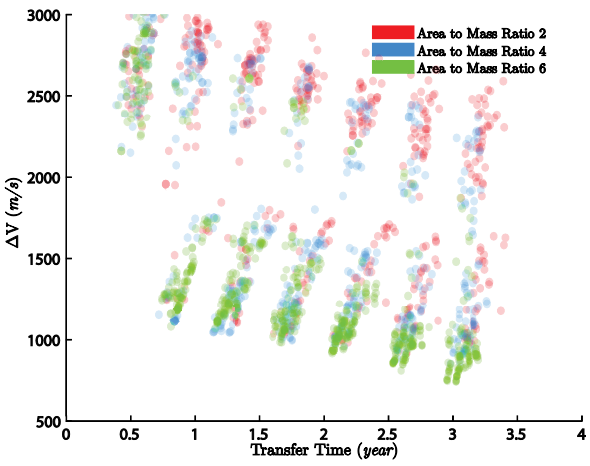

Fig. VII: Δv as a function of total transfer time of the solutions found for the large halo orbit.

The lowest scoring candidates for the large orbit for varying sailing periods and area-to-mass ratios are given in Table IV in m/s.

Sailing Period	AMR 2	4	6
0	2,311	2,150	2,160
0.5	1,244	1,111	1,081
1.0	1,105	1,046	1,072
1.5	1,034	997	985
2.0	984	960	916
2.5	913	883	812
3.0	936	854	747

Table IV: Lowest Δv solution found for the large halo orbit.

Some preliminary remarks can be made about the above results. It generally costs less to connect from an Earth GTO orbit to the larger halo orbits. Additionally, the spread of the solutions increases as the size of the halo orbit increases. Both these points make sense, as the manifold tubes for the larger halo orbits are much wider and allow for a far wider array of states to be used as connection points.

IV.II Low Cost Spacecraft

For the low cost spacecraft the same method is used to find possible transfers, a number of manifold lines on the manifold tube are used to attempt connection between halo and Earth enlarged GTO (cf. Fig. IV). Fig. VIII shows the resulting Δv costs for a connection between Earth enlarged GTO and a small planar halo orbit.

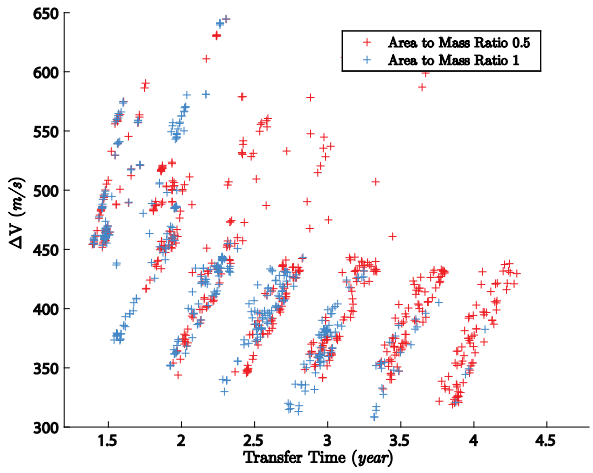

Fig. VIII: Δv as a function of total transfer time of the solutions found for the small halo orbit.

Fig. IX shows the resulting Δv costs for a connection between Earth enlarged GTO and a medium planar Halo orbit.

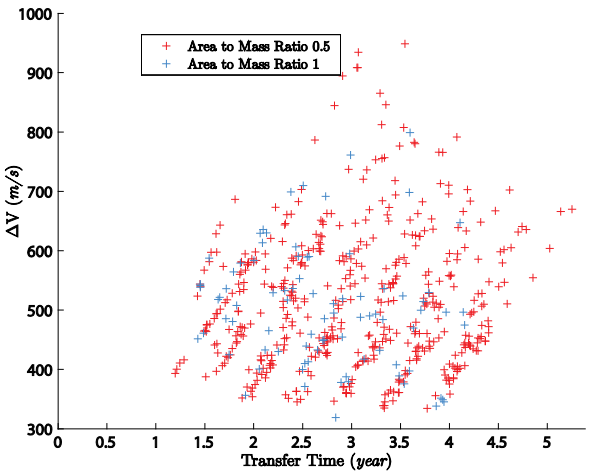

Fig. IX: Δv as a function of total transfer time of the solutions found for the medium halo orbit.

Fig. X shows the resulting Δv costs for a connection between Earth enlarged GTO and a large planar halo orbit.

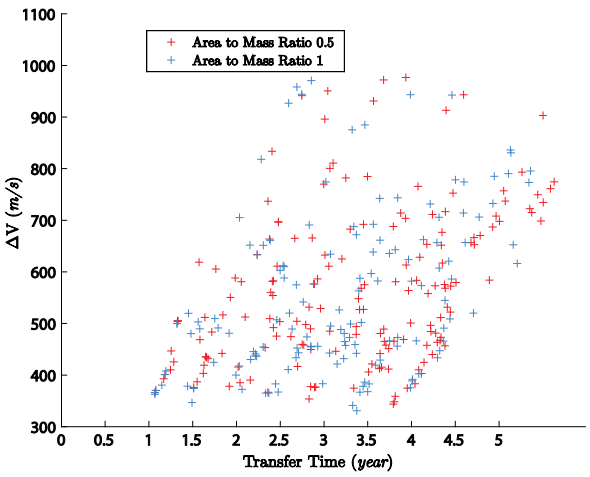

Fig. X: Δv as a function of total transfer time of the solutions found for the large halo orbit.

Note that one should add 1.9 km/s to the Δv figures shown in the above 3 graphs to arrive at the total cost. These results generally show the same trend as the previous solutions for the high performance spacecraft. The number of manifold lines extended from the halo orbit was smaller however, which likely explains the relatively poor performance of the area-to-mass ratio 1 values for the longer transfer times when compared to those with area-to-mass ratio 0.5 in Fig. IX and Fig. X.

Transfer Examples

Two examples of transfers with the low cost spacecraft are shown. The first can be viewed in Fig. XI. Manoeuvres are indicated in red dots, the black arcs are coasting sections of the transfer, while coloured arcs are manoeuvring sections where the reflective surface is uncontrolled.

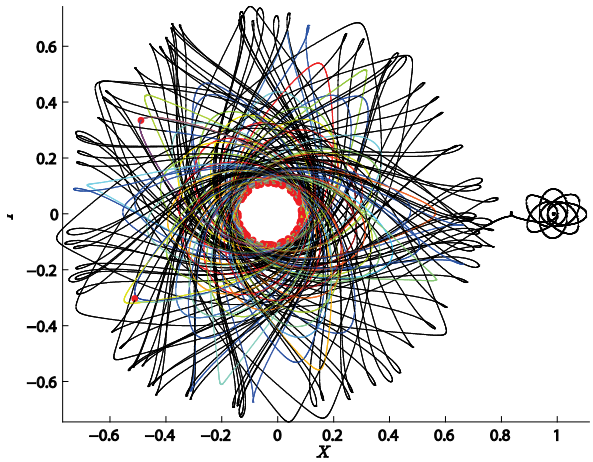

Fig. XI: Transfer from Earth enlarged GTO to small halo orbit with low cost spacecraft with manoeuvres modelled as 5 m/s impulses.

This transfer to a small halo orbit counts 64 manoeuvres, costing 313 m/s in total. Together with the initial constant thrust portion after GTO the total cost in Δv becomes 2.20 km/s. The coasting part of the transfer lasts for 734 days while the manoeuvring part lasts 289 days leading to a total transfer time of 1023 days. The additional cost to travel from small halo to quasi-capture about the Moon is neglible. The second example is shown in Fig. XII.

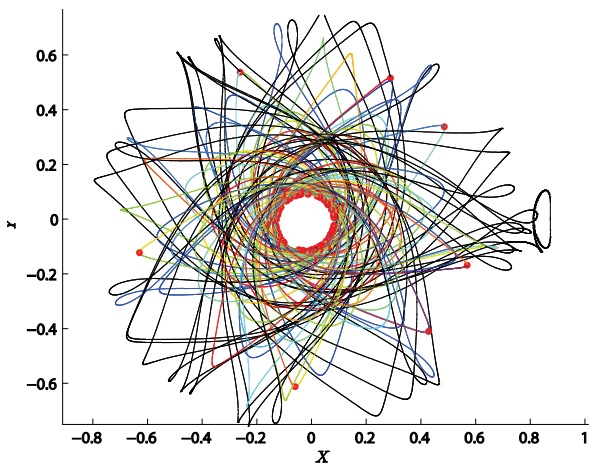

Fig. XII: : Transfer from Earth enlarged GTO to medium halo orbit with low cost spacecraft with manoeuvres modelled as 5 m/s impulses.

This transfer to medium halo orbit has 72 manoeuvres, costing 351 m/s. Together with the constant thrust arc to escape GTO quickly, the total Δv becomes 2.24 km/s. The coasting period where the reflective sail is used is 1 year, while the manoeuvring portion takes 336 days, leading to a total transfer time of 701 days. The additional cost to achieve quasi-capture is between 20 m/s and more, depending on the longevity of capture required.

V. MAPPING LUNAR ORBIT LONGEVITY

A study was undertaken to analyse what kind of conditions near the L1 libration point would be beneficial for longer duration quasi-periodic orbit about the Moon. To this end, a spacecraft (without reflective surface) is placed at positions at $x = x_{L1}$ and interspaced along $-0.25 < y < 0.25$. The spacecraft is then given an initial velocity of $\dot{y} = 0$ and $-0.2 < \dot{x} < 0.2$ (all values in the non-dimensional system). The state of the spacecraft can be written as

$$\boldsymbol{x}_{sc} = [x_{L1} \quad y \quad 0 \quad \dot{x} \quad 0 \quad 0]. \qquad [9]$$

Propagating this state forward using the variable stepsize Runge-Kutta 5th order (with embedded 4th order formula to estimate truncation error) method provided by MATLAB for up to a maximum of 3 years leads to the results presented in Fig. XIII (note that the orbit lifetime is presented in non-dimensional time units, where 250 units roughly equates to 3 years). In the following portion of the text 'stability' is mentioned several times. In the framework of this discussion, an orbit is considered stable when it fulfils

$$x_{L1} < x < x_{L2} \qquad [10]$$

and

$$\sqrt{x^2 + y^2} > R_{Moon}. \qquad [11]$$

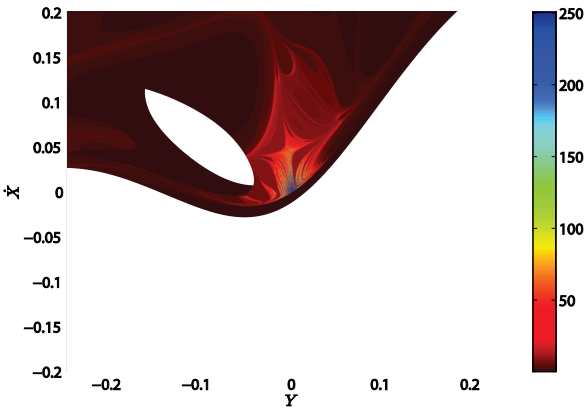

Fig. XIII: Spacecraft orbit longevity of up to 3 years based on the varying initial conditions of $\dot{x}$ and y.

Large swaths of the map are accompanied by a low lifetime. Naturally those areas with a negative $\dot{x}$ correspond to a rapid deterioration of the orbit. The central area, however, has several layers where the orbit lifetime is very high. A detailed view of this interesting region is shown in Fig. XIV.

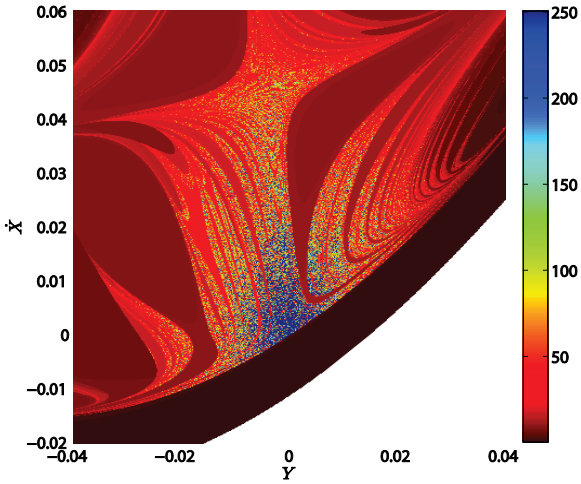

Fig. XIV: Detailed view of the central area of the spacecraft orbit longevity plot based on the varying initial conditions of $\dot{x}$ and y.

Fig. XV provides an overview of what causes the spacecraft orbit about the Moon to stop.

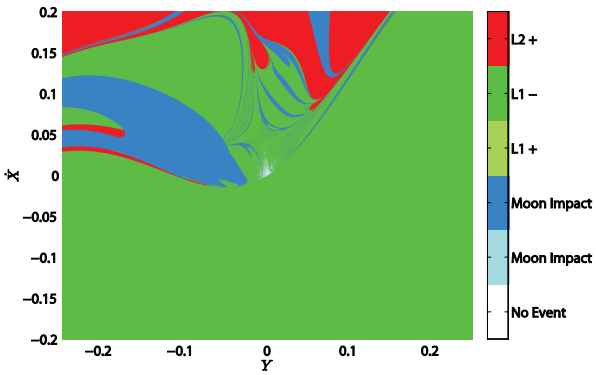

Fig. XV: Event causing the orbit propagation to halt based on the varying initial conditions of $\dot{x}$ and y.

The conditions listed on the colour-bar are 'No Event', meaning the orbit it stable, 'Moon Impact -', meaning the spacecraft eventually impacts the lunar surface, 'L1 -', meaning the spacecraft crosses out past x_{L1} towards the Earth again, and 'L2 +', meaning the spacecraft passes out past x_{L2}. Note that the 2 conditions listed as 'L1+' and 'Moon impact +' in the colour-bar in Fig. XV are not seen on the plot, as they are impossible. One involves impacting the lunar surface from within, and one involves passing the x_{L1} point from Earth to the Moon which cannot occur unless this point is passed from Moon to the Earth beforehand.

One final figure, Fig. XVI, shows the orbit longevity once again but with a maximum orbit lifetime of 3 months.

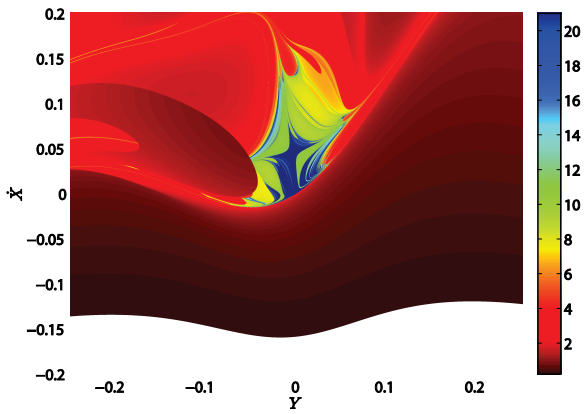

Fig. XVI: Spacecraft orbit longevity up to 3 months based on the varying initial conditions of $\dot{x}$ and y.

VI. CONCLUSIONS

A basic model has been built to explore the use of high area-to-mass ratio hybrid propulsion spacecraft in exploring the Moon. However, there still remain a great many improvements to be made to the overall method. The fidelity can be increased by converting impulses into thrusting arcs and to allow more freedom in the selection of manoeuvres. Also, the model should incorporate direct to Moon transfers without being inserted into halo orbit initially (generally a matter of scheduling a number of additional manoeuvres). The model as of yet only optimises the control of the reflective surface locally. Because of the nonlinearity of the system, it is likely that some improvement can be made when this is treated as a global optimisation problem. The lunar longevity plots show that small changes in velocity can make a large difference in determining the stability of the lunar orbit.

1. Simo, J. and McInnes, C.R., 2009: Solar sail orbits at the Earth-Moon libration points, Communications in Nonlinear Science and Numerical Simulations, pp. 4191-4196.
2. McInnes, C. R., 2004: Solar Sailing: Technology, Dynamics and Mission Applications. Berlin, Springer-Verlag.
3. Richardson, D.L., 1980: Analytic Construction of Periodic Orbits about the Collinear Points, Celestial Mechanics 22, pp 241-253.
4. Howell, K.C., 1984: Three-dimensional, periodic, 'halo' orbits, Celestial Mechanics 32, pp. 53-71.
5. Koon, W.S., Lo, M. W. Marsden, J. E., and Ross, S.D., 2007: Dynamical Systems, the three-body problem, and space mission design, New York, Springer-Verlag.